

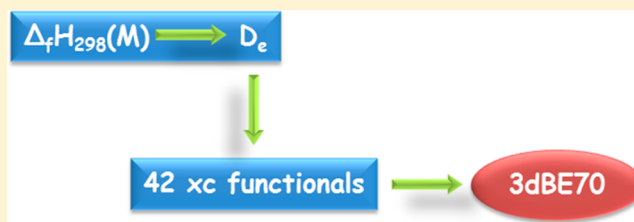
Tests of Exchange-Correlation Functional Approximations Against Reliable Experimental Data for Average Bond Energies of 3d Transition Metal Compounds

Wenjing Zhang,^{†,‡} Donald G. Truhlar,^{*,‡} and Mingsheng Tang[†]

[†]College of Chemistry and Molecular Engineering, Zhengzhou University, Zhengzhou, Henan Province 450001, P. R. China

[‡]Department of Chemistry and Supercomputing Institute, University of Minnesota, Minneapolis, Minnesota 55455-0431, United States

ABSTRACT: One of the greatest challenges for the theoretical study of transition-metal-containing compounds is the treatment of intrinsically multiconfigurational atoms and molecules, which require a multireference (MR) treatment in wave function theory. The accuracy of density functional theory for such systems is still being explored. Here, we continue that exploration by presenting the predictions of 42 exchange-correlation (xc) functionals of 11 types [local spin density approximation (LSDA), generalized gradient approximation (GGA), nonseparable gradient approximation (NGA), global-hybrid GGA, meta-GGA, meta-NGA, global-hybrid meta-GGA, range-separated hybrid GGA, range-separated hybrid meta-GGA, range-separated hybrid meta-NGA, and DFT augmented with molecular mechanics damped dispersion (DFT-D)]. DFT-D is tested both for Grimme's DFT-D3(BJ) model with Becke-Johnson damping and for ω B97X-D, which has the empirical atom–atom dispersion parametrized by Chai and Head-Gordon. The Hartree–Fock (HF) method has also been included because it can be viewed as a functional with 100% HF exchange and no correlation. These methods are tested against a database including 70 first-transition-row (3d) transition-metal-containing molecules (19 single-reference molecules and 51 MR molecules), all of which have estimated experimental uncertainties equal to or less than 2.0 kcal/mol in the heat of formation. We analyze the accuracy in terms of the atomization energy per bond instead of the enthalpy of formation of the molecule because it allows us to test electronic energies without the possibility of cancellation of errors in electronic energies with errors in vibrational energies. All the density functional and HF wave functions have been optimized to a stable solution, in which the spatial symmetry is allowed to be broken to minimize the energy to a stable solution. We find that τ -HCTHhyb has the smallest mean unsigned error (MUE) in average bond energy, in particular 2.5 kcal/mol, for the full set of 70 molecules, and it also gives the smallest MUE for MR systems. For single-reference systems, MPW1B95 has the best performance, with an MUE of 1.6 kcal/mol. Among local functionals, which are the least expensive, the best performance (MUE = 3.4 kcal/mol) for the total database is achieved by OreLYP. It is observed that adding HF exchange does not guarantee better accuracy for GGAs or for the NGA, but inclusion of the kinetic energy densities can benefit the GGAs and NGA calculations. The metal hydrides and metal oxides are demonstrated to be the most difficult bond types to predict, and CrO₃, FeH, CrO, VH, and MnS are found to be the most difficult molecules to predict. The middle transition metals (V, Cr, and Mn) lead to larger errors on average than either the early or late transition metals.



1. INTRODUCTION

The great popularity of density functional theory¹ (DFT) is due both to its practical usefulness and its contributions to fundamental understanding. However, DFT, being based on the electron density distribution $\rho(r)$, rather than the many-electron wave function, requires new modes of thinking about strategies for an accurate treatment of various kinds of bonds. Although DFT converts the primary focus from the Hilbert space of wave functions to the real space of $\rho(r)$, the most practical form of DFT, namely Kohn–Sham DFT,² still uses a single configuration of one-particle spin-orbitals in a noninteracting reference system to compute the dominant contribution to the kinetic energy, and this can be one of its chief limitations when treating systems whose wave functions are not well represented as a single antisymmetrized product of spin-orbitals—even though

Kohn–Sham theory is in principle exact for all systems, even for such inherently multiconfigurational systems. (We will use the convenient shorthand language of labeling inherently multiconfigurational systems as multireference systems and labeling systems whose wave functions are reasonably well represented by a single Slater determinant as single-reference systems.) Transition metal chemistry, which is key to most synthetic, industrial, and biological catalysts as well as to many energy conversion processes, is often dominated by multireference systems, and yet DFT is especially enticing for applications to complex catalytic systems because the shift of focus from the many-electron wave function to the density allows one to bypass

Received: May 21, 2013

Published: July 10, 2013

the high cost scaling³ of conventional wave function theory. (Both DFT and wave function methods can be improved in scaling using specially designed algorithms, but DFT is expected to remain relatively favorable in cost and even to become relatively more favorable in cost as system size increases.) We have learned that a good first step in improving DFT is achieving a better understanding of where the current theory is more successful or less successful, and with these considerations as motivation, the present work will pursue this issue for compounds containing 3d transition metals.

Kohn–Sham theory would be exact if we used the exact exchange–correlation (xc) functional, but it is unknown and essentially unknowable. Thus we must use approximations, and this is the chief limitation of the theory. Although there have been a large number of studies focusing on the accuracy of various xc functionals for the 3d or 4d transition metal dimers^{4–9} and small molecules and reactions,^{10–14} they are either inadequate in the variety of compounds (e.g., only homonuclear diatomics in ref 4) or in the type of xc functionals (e.g., only OLYP and O3LYP in ref 7). Many new xc functionals have been developed in recent years (e.g., M06, M11-L, and OreLYP – see below for references), and some of them (e.g., M06 and M11-L) have been validated to have broad accuracy for main-group molecules, but testing and validation of these approximate xc functionals for transition-metal molecules is more limited than for main-group molecules and solids, in part because of the scarcity of reliable data, such as bond enthalpies and heats of formation ($\Delta_f H$), to be used for such testing. In this regard, an important recent development is the database for transition metal molecules developed by Jiang et al.¹⁵ for use in testing composite wave function methods; this new database contains $\Delta_f H$ results for 225 3d-transition-metal-containing molecules. However, the inclusion of molecules with large experimental uncertainties is problematic and could lead to wrong conclusions; therefore, we will use a subset of 70 data judged to be most accurate.

This article is organized as follows. Section 2 specifies the xc functionals that are tested. Section 3 discusses the selection of data included in the database. Section 4 presents the theory and computational details. Section 5 gives the results and discussion, and Section 6 concludes the paper.

2. XC FUNCTIONALS

The xc functionals may be classified in terms of the ingredients upon which they are based.

The simplest xc functional is the local spin density approximation (LSDA) functional, in which the one includes exchange and correlation terms, each of which depends on only the spin-labeled electron densities, ρ_σ , where σ is α or β (i.e., spin-up or spin-down). When the reduced density gradients, s_σ , are also included, but the exchange term for each σ is a function of ρ_σ times a function of s_σ , the functional is called a generalized gradient approximation (GGA). If the term approximating exchange does not have this separable form, so that exchange and correlation are nonseparable, the resulting functionals will be called a nonseparable gradient approximation (NGA). (Even in a GGA, because the functionals are approximate and because the separation of exchange and correlation is not unique, the exchange term may include some correlation and the correlation term may include some exchange.) If the functional also depends on the spin-labeled kinetic energy densities, τ_σ , it is called a meta-GGA or meta-NGA.

The LSDAs, GGAs, NGAs, meta-GGAs, and meta-NGAs are all local functionals because the xc potential at a given spatial

coordinate depends only on functions (ρ_σ , s_σ , τ_σ) evaluated at that point. A fourth possible ingredient in xc functionals is the Hartree–Fock (HF) exchange energy density; the value of the quantity at any point in space depends on integrals of Kohn–Sham orbitals over the whole space; thus including HF exchange makes a functional nonlocal.

Functionals including HF exchange are called hybrid. If a hybrid functional is made by replacing a fixed percentage (i.e., a percentage independent of coordinates, ρ_σ , s_σ , τ_σ , or interelectronic separation) of local exchange by HF exchange, the functional is called a global hybrid, e.g., a global hybrid GGA, global hybrid meta-GGA, or global hybrid meta-NGA functional. If the HF exchange is introduced by partition the Coulomb operator into a long-range part and a short-range part and treating one of them by local exchange and the other by HF exchange, the functional is called a range-separated hybrid functional.

In some functionals, an empirical molecular mechanics (MM) term is added to the DFT energy to account for damped dispersion-like interactions, where the damping is due to overlap of subsystem charge distributions. This kind of functional is called a DFT-D functional.

Classified in the way just explained, the 42 density functionals studied here are listed in Table 1. The Hartree–Fock approximation is a wave function method and thus is not shown in Table 1. Nevertheless, we also include this approach in our study since it can be viewed as an approximate xc functional that has 100% HF exchange, no local exchange, and no correlation.

Table 1 gives the percentage X of HF exchange and the references^{2,10,16–51} for these functionals. There are eight GGAs, four meta-GGAs, eight global hybrid GGAs, 11 global hybrid meta-GGAs, two range-separated hybrid GGAs, four DFT-Ds, and one each of LSDA, NGA, meta-NGA, range-separated hybrid meta-GGA, and range-separated hybrid meta-NGA.

The specific reasons for choosing most of these xc functionals were discussed in our previous studies of p-block elements⁵² and 4d transition metal atoms;⁵³ in short functionals may have been selected for testing because they are historically important, popular, or expected to be especially accurate for one or another molecular property.

We also include some functionals that were not employed in either of the two studies mentioned in the previous paragraph, in particular (i) the Minnesota screened-exchange functional MN12-SX;⁴⁸ (ii) a functional, i.e., OreLYP, containing Thakkar's improved correlation functional (reLYP),²¹ that gives more accurate correlation energies for heavier atoms and atomic cations; (iii) three DFT-D functionals in which Grimme's D3(BJ)⁵⁰ model is used to add molecular mechanics damped dispersion to the OLYP, M06, and PW6B95 functionals; and (iv) two of the B97 series³³ of functionals. The rest of this section presents the motivations for adding these functionals to our survey.

The MN12-SX functional is constructed based on the nonseparable functional form introduced in N12²⁵ and MN12-L,³⁰ with addition of a portion of screened HF exchange that becomes local for large interelectronic separations. This functional has been demonstrated to be broadly accurate for chemistry and solid-state physics problems.

Thakkar et al. reparametrized xc functionals for the correlation energy in order to resolve the issue of poor performance for heavier atoms, in particular those with atomic number greater than 19. Although they concluded that the reparametrization has a limited effect on atomic energies, we believe it is interesting to

Table 1. Tested xc Functionals^a

type	name	X ^b	refs		type	name	X ^b	refs
LSDA	GKSVWN5 ^c	0	2, 16, 17			PBE0 ^f	25	36
GGA	BLYP	0	18, 19			SOGGA11-X	35.42	37
	MOHLYP	0	10	global hybrid meta-GGA		M05	28	38
	OHLYP	0	19, 20			M05-2X	56	39
	OLYP	0	19, 20			M06	27	40
	OreLYP ^d	0	19–21			M06-2X	54	40
	PBE ^e	0	22			M08-HX	52.23	41
	SOGGA	0	23			M08-SO	56.79	41
NGA	SOGGA11	0	24			MPW1B95	31	42
	N12	0	25			MPWB1K	44	42
meta-GGA	M06-L	0	26			PW6B95	28	43
	M11-L	0	27			TPSSH	10	44
	revTPSS	0	28			τ -HCTHhyb	15	29
	τ -HCTH	0	29	range-separated hybrid GGA		HSE	0–25	45, 46
meta-NGA	MN12-L	0	30			ω B97X	15.77–100	47
global hybrid GGA	B1LYP	25	31	range-separated hybrid meta-GGA		M11	42.8–100	49
	B3LYP	20	32	range-separated hybrid meta-NGA		MN12-SX	25–0	48
	B97-1	21	33	DFT-D		M06-D3(BJ) ^g	27	40, 50
	B97-3	26.93	34			OLYP-D3(BJ) ^g	0	19, 20, 50
	MPWLYP1M	5	10			PW6B95-D3(BJ) ^g	28	43, 50
	O3LYP	11.61	35			ω B97X-D	22.2–100	51

^aHartree–Fock is not listed here. ^bPercentage of HF exchange. ^cGáspár–Kohn–Sham for exchange and VWN5 for correlation (keyword SVWN5 in *Gaussian*). ^dOptX for exchange and reoptimized LYP for correlation. ^eAlso called PBEPPBE. ^fAlso known as PBEh, PBE1, or PBE1PBE. ^gDensity functional plus Grimme’s DFT-D3(BJ) dispersion correction.

include these functionals in evaluating xc functional performance for 3d transition metal compounds.

The latest version of Grimme’s DFT-D series for molecular mechanics damped dispersion additions to DFT calculations is called the DFT-D3(BJ) method. It is applicable to the whole periodic table of elements and sometimes achieves CCSD(T) accuracy for molecules.⁵⁰

In the B97 series of functionals, we tested both B97-1 and B97-3; the latter is an updated version of B97-1, and it has previously been shown to have good average performance for bond energies and barrier heights. (But in this present study, we will see that B97-1 performs slightly better than B97-3 in calculations on multireference molecules.)

3. DATABASE

When selecting data for a database, one must balance two competing demands, one for high accuracy data and one for making the database as broad and diverse as possible. For most transition-metal-containing molecules, accurate experimental energetic and geometrical quantities are unavailable, but an assessment depending on the experimental data with large uncertainties could lead to wrong conclusions. Many efforts have been made to evaluate the accuracy of DFT or other computational methods for calculations of 3d transition-metal-containing compounds,^{15,54–61} but the employed databases may be uncomprehensive because of, for example, exclusion of organometallics,⁵⁴ or the conclusions may be clouded by the involvement of a large number of molecules with large experimental uncertainties. With these two factors in mind, we take advantage of the efforts of Jiang et al., who presented estimated error bars for a large number of data, and in particular we included only the 70 data that they estimated¹⁵ to have experimental uncertainties equal to or less than 2.0 kcal/mol. This database involves all the 3d transition metals Sc, Ti, V, Cr, Mn, Fe, Co, Ni, Cu, and Zn and has great diversity in that it includes

compounds ranging from diatomics, such as hydrides, halides, and oxides, to simple clusters like (CuCl)₃ and to coordination complexes with organic ligands, for instance, ferrocene.

Table 2 lists the 70 molecules along with their average bond energies (*ABE*, converted from the experimental enthalpies of formation as explained in the following section) and experimental uncertainties for the enthalpies of formation. Based on Jiang et al. analysis,¹⁵ 51 of the 70 molecules show significant multireference character, and the remaining 19 molecules do not. In later sections, we will discuss the mean errors for these subdatabases as well as the mean errors for the total database.

4. THEORY AND COMPUTATIONAL DETAILS

4.1. Theory. We prefer to carry out our tests using the Born–Oppenheimer equilibrium atomization energy D_e rather than the enthalpy of formation, where D_e denotes the energy required to dissociate all bonds (atomization energy). The Born–Oppenheimer energy E is the sum of the electronic energy and the nuclear repulsion, and D_e is the sum of E for all atoms minus E for the molecule at the equilibrium geometry defined as the minimum of the potential energy curve (for diatomic molecules) or potential energy surface (for triatomic and larger molecules). The reason for preferring D_e to enthalpy of formation is that D_e does not involve the vibrational energy, and so the question of cancellation of errors in the electronic and vibrational energies does not arise. Also D_e does not involve atoms in their standard states, which are problematic since the standard state is often a solid rather than a gas-phase molecule, but we want to test the electronic structure methods in the absence of condensed-phase effects. Therefore, we first transform the best estimates of the experimental enthalpies of formation to reference values of D_e .

We will illustrate the procedure for a molecule *M* with formula A_xB_y ; the extension for ternary and more complex

Table 2. List of the Database Molecules with Average Bond Energies (ABE) and Experimental Uncertainties for the Enthalpies of Formation^b

molecule	ABE	uncertainty ^a	molecule	ABE	uncertainty ^a
Single-Reference					
TiCl ₂	111.1	2.0	CoBr ₂	82.2	1.1
VCl ₂	109.3	2.0	NiF ₂	111.4	1.1
CrCl ₂	91.4	0.4	Cu ₂	45.8	1.3
MnCl	81.6	1.6	ZnH	21.6	0.5
MnF ₂	116.5	1.0	ZnS	34.8	1.0
MnCl ₂	95.2	1.0	ZnSe	27.9	1.4
FeCl	80.5	1.6	ZnCl	54.3	1.0
FeCl ₂	96.6	1.0	ZnF ₂	94.8	1.1
FeBr ₂	85.5	0.5	ZnCl ₂	77.4	0.4
CoCl ₂	93.4	1.0			
Multireference					
Sc(C ₅ H ₅) ₃	78.7	1.4	Cr ₂	33.5	2.0
TiCl	102.3	2.0	MnS	71.0	2.0
TiCl ₃	108.4	2.0	Mn(CO) ₃ (C ₅ H ₅)	96.7	0.7
TiC ₄	83.9	0.5	FeH	40.1	1.9
TiCl ₄	104.1	0.7	FeCl ₃	83.6	1.0
TiBr ₄	91.6	0.2	FeBr ₃	73.9	1.0
Ti(C ₅ H ₅)Cl ₃	82.6	1.6	Fe(OH) ₂	103.6	0.5
VH	52.3	1.6	(FeCl ₂) ₂	70.7	1.0
VO	152.1	2.0	(FeBr ₂) ₂	63.8	1.9
VCl	103.7	2.0	(FeCl ₃) ₂	67.3	2.0
VCl ₃	99.8	2.0	Fe(CO) ₅	144.7	1.7
VCl ₄	92.6	0.6	Fe(C ₅ H ₅) ₂	78.5	0.6
VF ₅	113.4	0.2	CoCl	83.6	1.6
VOCl ₃	110.3	1.3	Co(CO) ₄	147.0	1.8
CrH	46.8	1.6	Co(CO) ₄ H	137.1	0.5
CrO	111.4	1.6	NiCl	91.6	1.0
CrCl	91.0	1.6	NiCl ₂	91.6	0.6
CrO ₂	119.7	1.2	Ni(CO) ₃	150.5	1.1
CrO ₃	118.1	1.0	Ni(CO) ₄	148.4	0.6
CrCl ₃	84.2	1.5	CuH	68.7	2.0
CrOH	96.6	1.8	CuCl	88.6	0.4
CrOF	124.1	1.9	(CuCl) ₃	43.8	0.5
CrO ₂ Cl ₂	100.3	1.0	ZnO	38.1	0.9
Cr(OH) ₂	101.7	1.2	Zn(CH ₃) ₂	88.6	0.3
CrO ₂ (OH) ₂	105.8	1.7	Zn(CH ₂ CH ₃) ₂	92.0	2.0
Cr(CO) ₆	145.1	1.1			

^aThe uncertainty listed is that in the heat of formation, from ref 15. ^bUnit: kcal/mol.

molecules should be obvious. The atomization energy D_e is defined as

$$D_e = xE(A) + yE(B) - E(A_xB_y) \quad (1)$$

We begin with the experimental enthalpy of formation $\Delta_f H_{298}(M)$ from the data collected by Jiang et al.,¹⁵ where the subscript 298 is an abbreviation of the standard temperature of 298.15 K. The first step is the transformation of this heat of formation from 298.15 to 0 K, which is done by the following equation⁶²

$$\Delta_f H_0(M) = \Delta_f H_{298}(M) - H_{\text{therm}}(M) + xH_{\text{therm}}(A_{\text{st}}) + yH_{\text{therm}}(B_{\text{st}}) \quad (2)$$

where $H_{\text{therm}}(M)$ is the positive difference between the enthalpy of the gas-phase molecule M at 298.15 K and that at 0 K, and where $H_{\text{therm}}(A_{\text{st}})$ is the positive difference between the enthalpy one mole of element A in its standard state at 298.15 K and that

at 0 K. Then we convert $\Delta_f H_0(M)$ to the enthalpy of atomization at 0 K (for all species in the gas phase) by

$$\Delta_a H_0(M) = x\Delta_f H_0(A) + y\Delta_f H_0(B) - \Delta_f H_0(M) \quad (3)$$

The values of $H_{\text{therm}}(A_{\text{st}})$, $H_{\text{therm}}(B_{\text{st}})$, $\Delta_f H_0(A)$, and $\Delta_f H_0(B)$, as obtained from standard thermodynamic sources,^{63–65} are tabulated in the Supporting Information of ref 15. For molecules we calculate $H_{\text{therm}}(M)$ by the *Gaussian 09* program⁶⁶ by using

$$H_{\text{therm}} = E_{\text{vib}} + E_{\text{rot}} + E_{\text{trans}} + k_B T - E_{\text{ZPE}} \quad (4)$$

where vib, rot, and trans denote vibrational, rotational, and translational energies, and E_{ZPE} is the zero-point energy. We calculate E_{rot} by the rigid rotator approximation, and we calculate E_{vib} and E_{ZPE} by a quasiharmonic approximation as discussed below. Note that E_{vib} includes zero point energy.

The atomization energy of molecule M at 0 K may also be denoted as $D_0(M)$ because it is the energy required for complete dissociation from the ground state, which is denoted

Table 3. Signed Errors (in kcal/mol) in ABE of Selected Molecules Calculated by the def2-TZVP–ma-TZVP Basis Set and the def2-QZVPP–ma-QZVPP Basis Set

molecule	def2-TZVP–ma-TZVP				def2-QZVPP–ma-QZVPP			
	M06-L	τ -HCTHhyb	B97-1	OreLYP	M06-L	τ -HCTHhyb	B97-1	OreLYP
FeCl ₂	6.5	1.3	0.3	−2.1	6.5	2.3	1.2	−1.2
TiCl ₂	7.3	−0.4	−1.5	−1.7	6.8	0.1	−1.1	−1.3
ZnH	−1.6	−1.5	−2.0	2.5	−1.6	−0.6	−1.4	3.3
Zn(CH ₃) ₂	−0.6	−1.1	−1.3	−0.2	−0.5	−0.8	−1.1	−0.1

by the subscript 0. The equilibrium dissociation energy is then given by

$$D_e(M) = D_0(M) + E_{ZPE} \quad (5)$$

Next we eliminate spin–orbit energy from D_e by

$$D_e^{xSO}(M) = D_e(M) - xE_{SO}(A) - yE_{SO}(B) \quad (6)$$

where xSO denotes exclusive of spin–orbit energy, and $E_{SO}(A)$ is a negative number representing the lowering of the energy of atom A due to spin–orbit coupling. We neglect the spin–orbit energies of the molecules, and atomic spin–orbit energies are obtained from experimental data (as tabulated in the Supporting Information of ref 15).

Finally, we calculate the average bond energy ABE , which is our reference quantity to compare the computational and experimental values, through the following equation

$$ABE(M) = D_e^{xSO}(M)/n_M \quad (7)$$

where n_M is the number of bonds in M (we count bonds, not bond orders, so a double bond still counts as one bond). To be consistent with this treatment, we will not include spin–orbit energy in the density functional calculations that we compare to $ABE(M)$.

We used density functional calculations with the M06-L xc functional (with a basis set described in Section 4.2 and with the scaling factor of 0.976⁶⁷) to determine the thermal contribution H_{therm} to the enthalpy and to determine the zero point energy, both of which are needed in the above transformation. This choice of density functional is based on previous tests showing that M06-L is among the most accurate functionals for transition metals^{26,52} and also that it has good accuracy for vibrational frequencies.⁴⁰ The use of a scale factor with calculated harmonic frequencies corrects for systematic errors in the harmonic frequencies and introduces anharmonicity in an average way; for the latter reason, the vibrational treatment is quasiharmonic, not harmonic.

4.2. Computational Details. All calculations were carried out nonrelativistically. All the density functional and Hartree–Fock (HF) wave functions have been optimized to a stable solution, which means the spatial symmetry is allowed to be completely broken to achieve a local minimum of the energy with respect to orbital variations (while, however, maintaining collinear, real orbitals).

For each molecule we first determined the spin multiplicity of the ground state by performing calculations of two or more spin states with the M06-L xc functional. One validation of this is that we found the M06-L functional predicts the correct ground state spin multiplicity for all atoms in this study. Furthermore, when we use M06-L to locate the most stable spin states, the results were found to be in agreement with Jiang et al.'s calculations⁶⁸ for all of the molecules. Therefore, we do not repeat the search for the lowest-energy spin state with all the other functionals.

All calculations in the present paper were carried out with a locally modified version of *Gaussian 09*.^{66,69} The geometry optimizations for all xc functionals and for the HF method were performed with a broken-symmetry calculation in which the orbitals were optimized (if instability is detected) until the wave function is stable. For integrals of the xc energy density, we used pruned grids with 99 radial shells and 590 angular points in each shell (which is called the “ultrafine” grid in *Gaussian 09*).

For the basis set, we choose the all-electron def2-TZVP basis set⁷⁰ for metals and hydrogen atoms and the all-electron minimally augmented ma-TZVP⁷¹ basis set for other atoms. The good performance of nonrelativistic def2-TZVP calculations is documented elsewhere,⁷² and our group has found that adding diffuse *s* and *p* functions on electronegative atoms (as is done in the minimally augmented basis set) is more efficient for increasing the accuracy of density functional calculations of barrier heights and electron affinities than either increasing the valence space ζ level or adding extra polarization functions (e.g., going from P-type to PP-type basis sets).⁷² However, to further validate our choice, for four molecules and four xc functionals we carried out a comparison of the present def2-TZVP–ma-TZVP choice to def2-QZVPP–ma-QZVPP calculations for the error in ABE . The results are shown in Table 3, which shows that the differences between the two basis sets are small and that using the larger basis set does not systematically improve the accuracy.

5. RESULTS AND DISCUSSION

We present both mean unsigned errors (MUEs) and mean signed errors (MSEs) of the average bond energies (ABEs) for the single-reference (SR) molecules, the multireference (MR) molecules, and for the total database of 70 molecules (which will be called the 3dBE70 database). Table 4 shows all the results with the functionals listed in order of increasing 3dBE70 MUE. Although the MUEs are our main criterion of accuracy, the MSEs are also shown to illustrate whether the average bond energies tend to be overestimated (positive) or underestimated (negative).

Table 4 shows that τ -HCTHhyb performs the best of all the tested functionals, i.e., it has the lowest 3dBE70 MUE, in particular 2.5 kcal/mol. The B97-1 and OreLYP functionals are the second and third best performing functionals, and they give MUEs of 2.7 and 3.4 kcal/mol, respectively, for 3dBE70. It is a pleasant surprise that the quite new functional OreLYP, which has not been widely studied, performs so well.

The LSDA, SOGGA, and OHLYP functionals are the only ones that give MUEs for 3dBE70 over 8 kcal/mol, although the HF wave function method also fails to do better than 8 kcal/mol. SOGGA was designed to illustrate the performance of a functional with a tight Lieb–Oxford bound that satisfies exactly the second-order gradient expansion; it was not designed to be a broadly accurate functional, and its poor performance for

Table 4. MUE and MSE of ABE over SR Molecules, MR Molecules, and the Total Database (3dBE70) for Each Functional, Sorted by Order of the 3dBE70 MUEs^b

name	X^a	MUE			MSE		
		SR	MR	3dBE70	SR	MR	3dBE70
τ -HCTHhyb	15	2.5	2.5	2.5	−0.3	0.7	0.4
B97-1	21	2.1	2.9	2.7	−0.9	−1.3	−1.2
OreLYP	0	3.8	3.2	3.4	−2.7	0.4	−0.4
MPWLYP1M	5	3.2	3.7	3.6	−1.9	1.7	0.7
ω B97X	15.77–100	2.6	4.2	3.7	−1.1	−2.3	−2.0
OLYP	0	4.2	3.8	3.9	−2.9	0.0	−0.9
M06-L	0	3.5	4.1	3.9	2.1	2.8	2.6
τ -HCTH	0	3.1	4.2	3.9	−0.2	3.1	2.2
ω B97X-D	22.2–100	2.2	4.5	3.9	−1.5	−3.0	−2.6
PW6B95-D3(BJ)	28	1.8	4.7	3.9	−0.7	−2.8	−2.3
OLYP-D3(BJ)	0	2.8	4.4	4.0	0.1	3.2	2.3
TPSSh	10	3.2	4.5	4.2	1.6	−0.1	0.3
PW6B95	28	2.0	5.1	4.2	−1.3	−3.4	−2.8
MPW1B95	31	1.6	5.2	4.3	−0.5	−3.5	−2.7
M06	27	5.0	4.1	4.4	−4.8	−2.6	−3.2
M06-D3(BJ)	27	5.0	4.1	4.4	−4.8	−2.6	−3.2
revTPSS	0	4.4	4.5	4.4	4.2	3.6	3.8
B97-3	26.93	2.6	5.1	4.4	−2.4	−3.8	−3.4
M11-L	0	5.8	4.0	4.5	3.6	1.6	2.2
MN12-L	0	4.8	4.4	4.5	2.3	2.1	2.2
BLYP	0	3.6	4.8	4.5	−2.2	2.5	1.2
M05	28	5.0	4.5	4.6	−4.4	−2.0	−2.7
PBE0	25	2.5	5.3	4.6	−0.4	−3.1	−2.3
HSE	0–25	3.1	5.6	4.9	−0.3	−3.4	−2.6
B3LYP	20	4.3	5.2	5.0	−3.9	−3.7	−3.7
O3LYP	11.61	4.5	5.3	5.1	−3.6	−3.0	−3.1
MOHLYP	0	5.9	4.9	5.2	−5.4	−1.9	−2.8
PBE	0	3.9	7.0	6.1	3.4	6.5	5.7
M08-HX	52.23	2.9	7.3	6.1	1.1	−6.2	−4.2
N12	0	6.3	6.2	6.2	5.4	5.1	5.2
M08-SO	56.79	3.0	7.7	6.4	−2.4	−6.7	−5.5
M05-2X	56	3.2	7.8	6.5	−1.9	−6.0	−4.9
M06-2X	54	3.1	8.0	6.7	−2.2	−6.3	−5.2
MPWB1K	44	2.3	8.4	6.8	−1.5	−7.6	−5.9
SOGGA11-X	35.42	4.6	7.8	6.9	−4.5	−7.3	−6.5
M11	42.8–100	8.6	6.4	7.0	7.0	−1.5	0.8
SOGGA11	0	8.4	7.0	7.4	6.2	5.6	5.8
B1LYP	25	6.0	8.0	7.5	−5.9	−6.9	−6.6
MN12-SX	25–0	10.8	6.8	7.9	7.6	1.8	3.4
OHLYP	0	11.1	12.0	11.8	−11.1	−11.3	−11.3
SOGGA	0	10.0	13.3	12.4	10.0	13.2	12.3
LSDA	0	17.1	23.2	21.5	17.1	23.2	21.5
HF	100	17.4	39.4	33.4	−15.2	−38.3	−32.1

^aPercentage of HF exchange. ^bUnit: kcal/mol.

bond energies is expected as a result of its small second order coefficient of the gradient enhancement, making it resemble the LSDA functional to a greater degree than the functionals found empirically to be more accurate for bond energies. OHLYP is a functional constructed by combining OptX exchange²⁰ with half of the LYP correlation¹⁹ instead of full LYP correlation. It is interesting to compare it to the closely related OLYP (which is like OHLYP but without the one-half), MOHLYP¹⁰ (which consists of modified OptX exchange and the half-LYP correlation), and OreLYP functionals, which perform very well.

For single-reference molecules, the most accurate functional turns out to be MPW1B95, which is a global hybrid meta-GGA

functional with 31% HF exchange; its MUE is only 1.6 kcal/mol. The next three best performing functionals for SR molecules are PW6B95-D3(BJ), PW6B95, and ω B97X-D, with MUEs of 1.8 kcal/mol, 2.0 kcal/mol, and 2.2 kcal/mol, respectively. M11 and MN12-SX give large MUEs of 8.6 and 10.8 kcal/mol, respectively, but they perform much better for systems with significant MR characteristics, with MUEs of 6.4 and 6.8 kcal/mol, respectively. The other functionals that are seen to have smaller MUEs for MR molecules than for SR molecules are the Minnesota functionals M05, M06, M11-L, and MN12-L, the Minnesota-developed functionals MOHLYP, N12, and SOGGA11, and the already mentioned OLYP and OreLYP functions.

Table 5. MUEs and MSEs of Each Functional and the Average Errors of Each Type of Functional, Arranged in Order of the Average MUEs over 3dBE70^b

type	name	X^a	MUE			MSE		
			SR	MR	3dBE70	SR	MR	3dBE70
DFT-D	ω B97X-D	22.2–100	2.2	4.5	3.9	−1.5	−3.0	−2.6
	PW6B95-D3(BJ)	28	1.8	4.7	3.9	−0.7	−2.8	−2.3
	OLYP-D3(BJ)	0	2.8	4.4	4.0	0.1	3.2	2.3
	M06-D3(BJ)	27	5.0	4.1	4.4	−4.8	−2.6	−3.2
average(4)			3.0	4.4	4.0	−1.7	−1.3	−1.4
meta-GGA	M06-L	0	3.5	4.1	3.9	2.1	2.8	2.6
	τ -HCTH	0	3.1	4.2	3.9	−0.2	3.1	2.2
	revTPSS	0	4.4	4.5	4.4	4.2	3.6	3.8
	M11-L	0	5.8	4.0	4.5	3.6	1.6	2.2
average (4)			4.2	4.2	4.2	2.4	2.8	2.7
range-separated hybrid GGA	ω B97X	15.77–100	2.6	4.2	3.7	−1.1	−2.3	−2.0
	HSE	25–0	3.1	5.6	4.9	−0.3	−3.4	−2.6
average (2)			2.9	4.9	4.3	−0.7	−2.9	−2.3
meta-NGA	MN12-L	0	4.8	4.4	4.5	2.3	2.1	2.2
global-hybrid GGA	B97-1	21	2.1	2.9	2.7	−0.9	−1.3	−1.2
	MPWLYP1M	5	3.2	3.7	3.6	−1.9	1.7	0.7
	B97-3	26.93	2.6	5.1	4.4	−2.4	−3.8	−3.4
	PBE0	25	2.5	5.3	4.6	−0.4	−3.1	−2.3
	B3LYP	20	4.3	5.2	5.0	−3.9	−3.7	−3.7
	O3LYP	11.61	4.5	5.3	5.1	−3.6	−3.0	−3.1
	SOGGA11-X	35.42	4.6	7.8	6.9	−4.5	−7.3	−6.5
	B1LYP	25	6.0	8.0	7.5	−5.9	−6.9	−6.6
average (8)			3.7	5.4	5.0	−2.9	−3.4	−3.3
global-hybrid meta-GGA	τ -HCTHhyb	15	2.5	2.5	2.5	−0.3	0.7	0.4
	TPSSH	10	3.2	4.5	4.2	1.6	−0.1	0.3
	PW6B95	28	2.0	5.1	4.2	−1.3	−3.4	−2.8
	MPW1B95	31	1.6	5.2	4.3	−0.5	−3.5	−2.7
	M06	27	5.0	4.1	4.4	−4.8	−2.6	−3.2
	M05	28	5.0	4.5	4.6	−4.4	−2.0	−2.7
	M08-HX	52.23	2.9	7.3	6.1	1.1	−6.2	−4.2
	M08-SO	56.79	3.0	7.7	6.4	−2.4	−6.7	−5.5
	M05-2X	56	3.2	7.8	6.5	−1.9	−6.0	−4.9
	M06-2X	54	3.1	8.0	6.7	−2.2	−6.3	−5.2
	MPWB1K	44	2.3	8.4	6.8	−1.5	−7.6	−5.9
average (11)			3.1	5.9	5.2	−1.5	−4.0	−3.3
NGA	N12	0	6.3	6.2	6.2	5.4	5.1	5.2
GGA	OreLYP	0	3.8	3.2	3.4	−2.7	0.4	−0.4
	OLYP	0	4.2	3.8	3.9	−2.9	0.0	−0.9
	BLYP	0	3.6	4.8	4.5	−2.2	2.5	1.2
	MOHLYP	0	5.9	4.9	5.2	−5.4	−1.9	−2.8
	PBE	0	3.9	7.0	6.1	3.4	6.5	5.7
	SOGGA11	0	8.4	7.0	7.4	6.2	5.6	5.8
	OHLYP	0	11.1	12.0	11.8	−11.1	−11.3	−11.3
	SOGGA	0	10.0	13.3	12.4	10.0	13.2	12.3
average (8)			6.4	7.0	6.8	−0.6	1.9	1.2
range-separated hybrid meta-GGA	M11	42.8–100	8.6	6.4	7.0	7.0	−1.5	0.8
range-separated hybrid meta-NGA	MN12-SX	25–0	10.8	6.8	7.9	7.6	1.8	3.4
LSDA	GKSVWN5	0	17.1	23.2	21.5	17.1	23.2	21.5
Hartree–Fock	HF	100	17.4	39.4	33.4	−15.2	−38.3	−32.1

^aPercentage of HF exchange. ^bUnit: kcal/mol.

For multireference molecules, the top three functionals are the same as those for the total database, i.e. τ -HCTHhyb, B97-1, and OreLYP, which have MUEs of 2.5, 2.9, and 3.2 kcal/mol, respectively. The only four entries with MUEs over 10 kcal/mol are SOGGA, OHLYP, HF, and LSDA. As we can see from Table 4, the MUEs of 3dBE70 have roughly the same trend as that of MR molecules, perhaps because

there are twice as many MR molecules as SR ones in the total database.

Table 5 shows the MUE and MSE analysis based on the classification of the functionals. We see that, with one exception, functionals with 0 to 15% HF exchange have positive MSEs (tend to overestimate bond energies), whereas those with 20 or more % HF exchange or with range separation have negative

Table 6. Average MUEs $[\text{MUE}_{\text{ave}}(B)]^a$ for Various Bond Types B in Each Class of Molecules^{bc}

	B1LYP	B3LYP	B97-1	B97-3	BLYP	HF	HSE	LSDA	M05	M05-2X	M06
Single-Reference Molecules											
M-H (1)	0.5	1.0	2.0	0.9	0.8	2.2	10.3	7.0	7.0	2.4	6.5
M-X (15)	6.2	4.5	2.4	2.7	4.0	18.3	2.7	17.8	4.8	3.5	4.9
M-S (1)	8.8	6.3	0.2	1.5	4.1	18.8	2.3	18.0	6.5	1.5	6.5
M-Se (1)	5.8	3.7	0.5	2.5	2.1	15.1	0.7	18.8	8.7	1.3	7.7
M-M (1)	6.2	4.3	2.1	3.3	0.3	21.0	4.9	13.5	1.9	3.2	1.1
Multireference Molecules											
M-H (4)	9.5	11.0	8.3	9.0	12.4	23.0	9.8	18.6	7.8	6.9	5.6
M-O (9)	11.6	6.4	5.2	9.1	7.1	64.9	11.2	29.9	8.1	13.7	9.7
M-C (7)	6.7	3.5	1.6	3.4	1.7	46.2	2.9	23.8	2.9	5.6	1.9
M-X (21)	6.4	4.3	1.8	3.6	3.3	25.9	3.2	19.2	3.1	4.7	2.6
M-Cy (2)	3.0	1.5	0.6	0.9	1.4	21.5	0.3	13.0	0.7	0.9	0.6
M-M (1)	10.2	9.5	1.7	0.1	10.9	31.9	14.9	34.8	5.9	18.7	2.3
M-L (7)	10.1	5.9	3.3	6.9	3.3	57.4	7.2	25.1	4.5	10.7	4.8
Total Database (3dBE70)											
M-H (5)	7.7	9.0	7.0	7.4	10.1	18.9	9.9	16.2	7.6	6.0	5.8
M-O (9)	11.6	6.4	5.2	9.1	7.1	64.9	11.2	29.9	8.1	13.7	9.7
M-C (7)	6.7	3.5	1.6	3.4	1.7	46.2	2.9	23.8	2.9	5.6	1.9
M-X (36)	6.3	4.4	2.0	3.2	3.6	22.7	3.0	18.6	3.8	4.2	3.5
M-Cy (2)	3.0	1.5	0.6	0.9	1.4	21.5	0.3	13.0	0.7	0.9	0.6
M-S (1)	8.8	6.3	0.2	1.5	4.1	18.8	2.3	18.0	6.5	1.5	6.5
M-Se (1)	5.8	3.7	0.5	2.5	2.1	15.1	0.7	18.8	8.7	1.3	7.7
M-M (2)	8.2	6.9	1.9	1.7	5.6	26.5	9.9	24.2	3.9	11.0	1.7
M-L (7)	10.1	5.9	3.3	6.9	3.3	57.4	7.2	25.1	4.5	10.7	4.8
	M06-2X	M06-D3(BJ)	M06-L	M08-HX	M08-SO	M11	M11-L	MN12-L	MN12-SX	MOHLYP	MPW1B95
Single-Reference Molecules											
M-H (1)	1.8	6.5	1.6	4.9	0.1	12.2	4.1	4.6	4.6	2.9	1.2
M-X (15)	2.8	4.9	3.8	2.3	3.4	7.9	5.4	4.5	12.1	6.0	1.7
M-S (1)	2.3	6.5	1.7	1.2	3.1	6.4	7.6	1.9	0.5	4.7	0.2
M-Se (1)	4.9	7.7	0.1	8.6	1.8	14.0	16.3	7.5	4.0	5.8	1.4
M-M (1)	8.1	1.1	5.2	4.8	0.9	11.8	0.9	9.2	14.4	7.7	3.7
Multireference Molecules											
M-H (4)	8.2	5.6	8.8	6.5	5.8	14.4	10.8	12.5	12.8	12.5	8.7
M-O (9)	12.9	9.7	2.5	14.8	16.2	9.8	3.0	4.3	6.5	3.7	10.6
M-C (7)	5.8	1.9	1.1	5.7	5.2	3.9	2.3	0.9	2.2	3.3	2.7
M-X (21)	5.3	2.6	5.0	3.6	4.3	3.3	3.4	3.9	5.3	5.0	2.8
M-Cy (2)	0.9	0.6	0.6	0.9	1.3	0.5	0.4	0.7	0.5	2.8	0.5
M-M (1)	15.5	2.3	8.8	3.9	3.5	19.6	9.0	17.6	37.3	5.7	14.8
M-L (7)	11.3	4.8	2.2	12.7	13.0	8.0	2.1	1.8	2.9	2.3	7.5
Total Database (3dBE70)											
M-H (5)	6.9	5.8	7.3	6.2	4.6	13.9	9.5	10.9	11.1	10.6	7.2
M-O (9)	12.9	9.7	2.5	14.8	16.2	9.8	3.0	4.3	6.5	3.7	10.6
M-C (7)	5.8	1.9	1.1	5.7	5.2	3.9	2.3	0.9	2.2	3.3	2.7
M-X (36)	4.3	3.5	4.5	3.1	3.9	5.2	4.2	4.2	8.1	5.4	2.3
M-Cy (2)	0.9	0.6	0.6	0.9	1.3	0.5	0.4	0.7	0.5	2.8	0.5
M-S (1)	2.3	6.5	1.7	1.2	3.1	6.4	7.6	1.9	0.5	4.7	0.2
M-Se (1)	4.9	7.7	0.1	8.6	1.8	14.0	16.3	7.5	4.0	5.8	1.4
M-M (2)	11.8	1.7	7.0	4.4	2.2	15.7	5.0	13.4	25.9	6.7	9.3
M-L (7)	11.3	4.8	2.2	12.7	13.0	8.0	2.1	1.8	2.9	2.3	7.5
	MPWB1K	MPWLYP1M	N12	O3LYP	OHLYP	OLYP	OLYP-D3(BJ)	OreLYP	PBE	PBE0	PW6B95
Single-Reference Molecules											
M-H (1)	2.2	0.5	3.1	3.3	2.5	2.5	4.2	2.5	0.7	2.3	0.7
M-X (15)	2.1	3.7	6.4	4.3	11.1	4.2	2.9	4.1	4.2	2.6	2.1
M-S (1)	2.1	3.8	6.2	4.0	13.0	2.6	1.2	1.8	3.3	1.4	1.5
M-Se (1)	0.0	1.6	8.5	4.6	13.8	4.2	0.4	2.9	4.3	0.6	0.3
M-M (1)	6.8	0.4	5.4	8.7	15.5	7.5	4.8	4.3	2.4	5.2	2.9
Multireference Molecules											
M-H (4)	6.3	12.3	11.7	12.0	9.3	12.3	13.3	12.7	11.9	9.8	9.4
M-O (9)	18.8	5.0	5.1	6.6	14.9	3.4	4.0	3.0	8.8	10.0	9.5
M-C (7)	5.8	1.2	1.1	3.0	13.1	1.4	2.4	1.0	6.1	2.7	2.8

Table 6. continued

	MPWB1K	MPWLYP1M	N12	O3LYP	OHLYP	OLYP	OLYP-D3(BJ)	OreLYP	PBE	PBE0	PW6B95
Multireference Molecules											
M-X (21)	4.4	2.9	6.7	4.5	11.0	3.7	3.5	2.9	5.0	3.1	3.0
M-Cy (2)	0.5	0.9	0.8	0.8	9.1	0.8	1.8	0.3	2.5	0.6	0.2
M-M (1)	16.8	2.1	13.0	8.9	19.5	5.2	0.4	0.7	0.9	14.9	12.6
M-L (7)	13.5	2.0	3.5	5.3	13.8	1.0	3.2	1.0	6.8	7.2	6.8
Total Database (3dBE70)											
M-H (5)	5.5	9.9	10.0	10.2	8.0	10.4	11.5	10.6	9.7	8.3	7.7
M-O (9)	18.8	5.0	5.1	6.6	14.9	3.4	4.0	3.0	8.8	10.0	9.5
M-C (7)	5.8	1.2	1.1	3.0	13.1	1.4	2.4	1.0	6.1	2.7	2.8
M-X (36)	3.5	3.2	6.6	4.4	11.0	3.9	3.2	3.4	4.7	2.9	2.7
M-Cy (2)	0.5	0.9	0.8	0.8	9.1	0.8	1.8	0.3	2.5	0.6	0.2
M-S (1)	2.1	3.8	6.2	4.0	13.0	2.6	1.2	1.8	3.3	1.4	1.5
M-Se (1)	0.0	1.6	8.5	4.6	13.8	4.2	0.4	2.9	4.3	0.6	0.3
M-M (2)	11.8	1.3	9.2	8.8	17.5	6.4	2.6	2.5	1.7	10.1	7.8
L1-M-L2 (7)	13.5	2.0	3.5	5.3	13.8	1.0	3.2	1.0	6.8	7.2	6.8
	PW6B95 -D3(BJ)	revTPSS	SOGGA	SOGGA11	SOGGA11-X	τ -HCTH	τ -HCTHhyb	TPSSH	ω B97X	ω B97X-D	
Single-Reference Molecules											
M-H (1)	0.8	7.8	3.2	2.7	1.8	2.1	1.5	7.2	1.5	1.4	
M-X (15)	1.9	4.0	10.5	6.9	4.8	3.5	2.5	3.2	2.3	2.1	
M-S (1)	0.8	4.1	11.6	14.5	6.4	1.3	0.7	0.8	6.5	4.9	
M-Se (1)	1.1	7.1	12.1	22.0	4.3	0.8	2.1	3.5	4.4	3.5	
M-M (1)	2.2	3.5	6.0	18.2	1.3	3.8	5.8	2.0	2.5	0.3	
Multireference Molecules											
M-H (4)	9.5	14.6	12.3	13.2	4.0	14.9	9.9	13.6	8.5	8.7	
M-O (9)	9.3	3.9	15.9	8.2	16.5	3.4	2.4	6.1	7.4	8.5	
M-C (7)	2.5	0.8	13.4	3.2	4.7	0.9	0.9	2.9	2.4	2.7	
M-X (21)	2.4	4.1	11.4	6.3	5.3	3.2	1.7	2.8	2.6	2.4	
M-Cy (2)	0.4	0.6	7.0	0.8	0.7	0.6	0.4	0.1	0.4	0.4	
M-M (1)	10.9	4.2	4.9	4.9	7.1	38.8	10.4	9.7	0.9	11.6	
M-L (7)	6.5	2.4	13.8	5.7	11.2	1.5	1.3	3.3	5.1	5.8	
Total Database (3dBE70)											
M-H (5)	7.7	13.3	10.5	11.1	3.5	12.3	8.2	12.3	7.1	7.2	
M-O (9)	9.3	3.9	15.9	8.2	16.5	3.4	2.4	6.1	7.4	8.5	
M-C (7)	2.5	0.8	13.4	3.2	4.7	0.9	0.9	2.9	2.4	2.7	
M-X (36)	2.2	4.1	11.1	6.6	5.1	3.3	2.1	3.0	2.5	2.3	
M-Cy (2)	0.4	0.6	7.0	0.8	0.7	0.6	0.4	0.1	0.4	0.4	
M-S (1)	0.8	4.1	11.6	14.5	6.4	1.3	0.7	0.8	6.5	4.9	
M-Se (1)	1.1	7.1	12.1	22.0	4.3	0.8	2.1	3.5	4.4	3.5	
M-M (2)	6.6	3.9	5.5	11.6	4.2	21.3	8.1	5.9	1.7	6.0	
M-L (7)	6.5	2.4	13.8	5.7	11.2	1.5	1.3	3.3	5.1	5.8	

^aMUE_{ave}(B) = $[\sum_{i=1}^m \text{MUE}_{i,B}]/m$, where m is the number of molecules that contain bond type B. ^bThere are no single-reference molecules in the M-O, M-C, M-Cy, or M-L subgroups and no multireference molecules in the M-S and M-Se subgroups. ^cUnit: kcal/mol.

MSEs (tend to underestimate bond energies). The one exception is O3LYP, with 11.61% HF exchange and a 3dBE70 MSE of -3.1 kcal/mol. The trends are consistent with the quite negative MSE given by the HF method, which has 100% HF exchange and no correlation.

For DFT-D methods, the parameters in the term that nominally represents damped dispersion are determined empirically for a given xc functional; therefore, the damped dispersion term may also make up for systematic errors (e.g., too much exchange repulsion) in a given xc functional to which it is added, and in the case of adding it to an xc functional that already includes damped dispersion, the added term may be very small, accounting only for the missing part of the damped dispersion. Tables 4 and 5 show that in the three D3(BJ) cases where we can compare the same functional with and without molecular mechanics damped dispersion, the results are very similar, although in two cases out of three the results actually get worse

with the added terms. Note that ω B97X and ω B97X-D differ in almost all of their parameters, not just by the addition of molecular mechanics damped dispersion.

The classes of functionals in Table 5 are arranged in order of increasing average 3dBE70 MUE. The table shows that meta-GGAs and the meta-NGA are much more accurate than the GGA and NGA, which indicates that the inclusion of kinetic energy density is efficacious for both GGA and NGA xc functionals. However, the addition of HF exchange to the GGA xc functionals is less successful. For the NGA families, the meta-NGA is demonstrated to be much better than the NGA or the range-separated hybrid meta-NGA.

It is interesting to look at the errors as a function of bond type. Hence we classify the total database into 9 subdatabases based on the kind of atoms bonded to the metal atoms. We label the nine types of bonding as M-H, M-C, M-O, M-X, M-Cy, M-S, M-Se, M-M, and M-L, where M represents a 3d transition metal;

Table 7. Average MUEs and MSEs [$\text{MUE}_{\text{ave}}(\text{M})$ and $\text{MSE}_{\text{ave}}(\text{M})$]^a of ABE for Every Molecule M

molecule	$\text{MUE}_{\text{ave}}(\text{M})$	$\text{MSE}_{\text{ave}}(\text{M})$	molecule	$\text{MUE}_{\text{ave}}(\text{M})$	$\text{MSE}_{\text{ave}}(\text{M})$	molecule	$\text{MUE}_{\text{ave}}(\text{M})$	$\text{MSE}_{\text{ave}}(\text{M})$
Single-Reference								
FeCl ₂	2.7	0.0	VCl ₂	3.6	−1.4	ZnCl	5.0	−3.6
TiCl ₂	2.9	−0.1	ZnF ₂	3.8	−2.0	ZnSe	5.1	0.4
ZnH	3.2	1.0	ZnS	4.1	−1.1	NiF ₂	6.0	−5.5
ZnCl ₂	3.3	−1.5	MnCl ₂	4.2	1.1	FeCl	6.9	5.3
CoBr ₂	3.5	−1.1	CrCl ₂	4.3	−1.6	MnCl	7.5	1.4
CoCl ₂	3.5	−1.9	MnF ₂	4.9	3.0			
FeBr ₂	3.6	−0.4	Cu ₂	5.0	−1.8			
Multireference								
Sc(C ₅ H ₅) ₃	1.0	−0.3	CrCl	4.1	0.4	TiCl	5.9	3.8
Zn(CH ₂ CH ₃) ₂	1.1	−0.7	TiBr ₄	4.1	−1.1	VOCl ₃	6.9	−4.1
Zn(CH ₃) ₂	1.2	−0.8	FeBr ₃	4.1	−1.9	CrO ₂ (OH) ₂	7.0	−4.5
Ti(C ₅ H ₅)Cl ₃	1.4	0.2	Cr(CO) ₆	4.1	−2.2	CuH	7.0	−6.8
Fe(C ₅ H ₅) ₂	1.4	−0.4	VCl ₄	4.2	−0.2	CoCl	7.2	5.5
Mn(CO) ₃ (C ₅ H ₅)	2.3	−0.6	CrCl ₃	4.2	−0.8	ZnO	7.5	−5.8
TiC ₄	2.4	1.2	Fe(OH) ₂	4.3	−3.8	CrH	8.0	7.8
(FeCl ₂) ₂	2.4	−1.4	Co(CO) ₄ H	4.5	−2.2	CrO ₂ Cl ₂	9.7	−6.1
(CuCl) ₃	2.8	−2.3	NiCl	4.5	−3.1	Cr ₂	10.0	−0.2
CrOH	2.9	−1.5	Fe(CO) ₅	4.7	−1.3	CrOF	10.3	−9.0
TiCl ₃	3.0	0.6	Co(CO) ₄	4.8	−2.8	CrO ₂	11.4	−6.8
(FeCl ₃) ₂	3.0	−1.5	CuCl	4.8	−3.3	VO	12.0	0.2
(FeBr ₂) ₂	3.2	−1.9	Ni(CO) ₄	5.0	−3.3	MnS	12.1	7.3
VCl ₃	3.4	−0.1	VCl	5.2	1.8	VH	12.7	12.5
FeCl ₃	3.4	−0.9	Ni(CO) ₃	5.4	−3.6	CrO	12.9	−10.4
TiCl ₄	3.9	−0.1	NiCl ₂	5.4	−4.8	FeH	12.9	12.6
Cr(OH) ₂	4.0	−3.6	VF ₅	5.6	0.2	CrO ₃	14.3	−10.0

^a $\text{MUE}_{\text{ave}}(\text{M}) = ((\sum \text{MUE})/(\# \text{ of functionals}))$; $\text{MSE}_{\text{ave}}(\text{M}) = ((\sum \text{MSE})/(\# \text{ of functionals}))$.

H, O, S, and Se are respectively hydrogen (hydrides), oxygen (including mono-, di-, and tri-oxides), sulfur (sulfides), and selenium atoms (selenides); X represents a halogen atom (fluorides, chlorides, and bromides); C represents noncyclic carbon (metal carbides and metal carbonyls), and Cy denotes cyclopentadiene (compounds with cyclopentadiene as the only kind of ligand); and L means ligand in all molecules involving two or more different types of metal bonds. M-M denotes a metal dimer. Table 6 shows the average MUEs of each group calculated by various xc functionals and the HF method. The numbers of molecules included in each group are given in parentheses. It turns out that MUEs of SR molecules are generally smaller than those of the molecules with significant MR character, while the total database accuracy of a functional is generally dominated by how well or poorly it can do in the MR molecules. For most functionals, the errors are large for M-H and M-O groups, which may partly be because most (M-H) or all (M-O) molecules of these groups belong to the MR subdatabase; the computational results for M-C, M-X, and M-Cy groups are much closer to the experimental results. In particular, averaged over all 42 xc functionals, the average MUE for the M-H and M-O groups are respectively 8.8 and 8.4 kcal/mol, whereas the average MUE for M-C, M-X, and M-Cy groups are respectively 3.3, 4.3, and 1.3 kcal/mol. To understand the very small number for M-Cy compounds, note that most of the bonds in these compounds do not involve the metal.

It is also interesting to identify "difficult" molecules. Table 7 displays the average MUEs and MSEs of ABE for every molecule, where the average is over all xc functionals that we tested except LSDA. The HF method is also excluded from the averages. The LSDA and HF methods are excluded from this statistic since they are presented simply for reference, not because they provide potential functionals for state-of-the-art applications. Table 7

shows that the most difficult SR molecules are three metal halides MnCl, FeCl, and NiF₂, which have average MUEs of 7.5 kcal/mol, 6.9 kcal/mol, and 6.0 kcal/mol, respectively. For MR molecules, the xc functionals perform best (on average) for the complex compounds Sc(C₅H₅)₃, Zn(CH₂CH₃)₂, and Zn(CH₃)₂. The most difficult MR molecules are found to be two oxides CrO₃ and CrO, along with a hydride FeH, with MUEs of 14.3, 12.9, and 12.9 kcal/mol, respectively. It will be interesting in future work to explore the features of these molecules that make them so difficult.

Another important issue is whether these functionals perform equally well (or poorly) for the late transition metal compounds as for the early ones. In posing this question, we note that there is more than one way to divide a transition metal series. The simplest is to label groups 3–7 (that is, Sc to Mn) as early and to label groups 8–12 (that is, Fe to Zn) as late. A more sophisticated method is to label groups 3 and 4 (Sc and Ti) as early, groups 5–7 (V to Mn) as middle, groups 8–11 (Fe to Cu) as late, and group 12 (Zn) as not being a transition metal at all since it does not have a partially filled d subshell. Table 8 examines the

Table 8. Average MUEs and MSEs [$\text{AMUE}(\text{G})$ and $\text{AMSE}(\text{G})$] of ABE for Every Transition Metal Group (G)^{a,b}

	early-late		early-middle-late-Zn			
	Sc–Mn	Fe–Zn	Sc–Ti	V–Mn	Fe–Cu	Zn
N_{molec}	35	35	8	27	26	9
AMUE(G)	6.2	4.5	3.1	7.1	4.7	3.8
AMSE(G)	−0.7	−1.3	0.5	−1.0	−1.3	−1.6

^a N_{molec} is the number of molecules in each group ^b $\text{AMUE}(\text{G}) = ((\sum \text{MUE})/(\# \text{ of functionals} \times N_{\text{molec}}))$; $\text{AMSE}(\text{G}) = ((\sum \text{MSE})/(\# \text{ of functionals} \times N_{\text{molec}}))$.

Table 9. MUE of Selected Functionals on a Broader Set of Data^a

name	X	3dBE70	HTBH38	ABDE12	PPSS	sum
ω B97X	15.77–100	3.7	2.0	4.4	0.3	10.4
M06	27	4.4	2.0	4.1	0.2	10.7
MN12-L	0	4.5	1.3	4.8	0.3	10.9
ω B97X-D	22.2–100	3.9	2.4	4.5	0.7	11.5
M11-L	0	4.5	1.4	6.4	0.4	12.7
MPW1B95	31	4.3	3.0	4.6	1.1	13.0
PW6B95	28	4.2	3.1	5.4	0.8	13.5
M05	28	4.6	1.9	7.8	1.0	15.3
B97-3	26.93	4.4	2.3	6.7	2.3	15.7
M06-L	0	3.9	4.1	7.7	0.2	15.9
τ -HCTHhyb	15	2.5	5.3	6.4	2.2	16.4
PBE0	25	4.6	4.2	7.1	1.7	17.6
HSE	0–25	4.9	4.2	7.7	1.6	18.4
B3LYP	20	5.0	4.2	9.8	2.9	21.9
revTPSS	0	4.4	7.0	8.6	2.4	22.4
TPSSh	10	4.2	6.0	10.5	2.5	23.2
τ -HCTH	0	3.9	6.9	9.9	2.6	23.3
MPWLYP1M	5	3.6	7.5	9.8	2.7	23.6
OLYP	0	3.9	5.6	11.5	5.0	26.0
BLYP	0	4.5	7.5	11.7	4.0	27.7

^aUnit: kcal/mol.

question from both of these points of view by showing the statistical results of the average MUEs and MSEs of ABE over the variously defined groups of transition metal compounds. The number of molecules included in each group is given in the first row (N_{molec}). We can observe that the average error for the late transition metal compounds is less than 5.0 kcal/mol by either definition of "late", but the error is slightly larger (7.1 kcal/mol) for the middle transition metals. This is opposite to the results of Ziegler and Li,⁷³ who found the DFT methods predict more accurate bond energies of early transition metal hydride cations (MH^+) than of the late ones. This can be attributed both to the different varieties of xc functionals we test and the much broader kinds of metal-containing compounds we calculate. From the more detailed results of a second method of dividing transition metals, we can account that the bigger errors for early transition metal compounds are mainly due to the poor performance for the V to Mn group of compounds. The mean signed errors are also interesting in that Table 8 shows that the Sc and Ti group is the only group for which the density functionals tend to overestimate bond energies.

The ultimate goal is to obtain a functional with universally good performance for a large number of properties. Many of the functionals tested here have also been tested more broadly, but in the present study, the frustrating trend that no one functional is satisfactory for the full range of experimental data is verified to still persist. For example, Barden and co-workers⁴ have concluded that local xc functionals (those with no HF exchange) often perform significantly better than hybrid ones in predicting properties of homonuclear 3d transition metal diatomics, but Yanagisawa and co-workers⁵ reported that the local xc functionals tend to overestimate the binding energies of 3d transition metal dimers, and the hybrid xc functionals give more accurate predictions. According to our study, however, those xc functionals with 0 to 15% HF exchange tend to give positive MSEs (with the only exception being O3LYP), and those with 20% or more HF exchange give negative MSEs. Nevertheless, it is possible to draw some broad conclusions. For example, B97-1 is found to be one of the most promising functionals both in the

studies of Jiang et al.⁶⁸ and in our work reported here; in particular, Jiang and co-workers found that B97-1 performs overall best among the 13 density functionals they tested to predict the thermochemistry of 193 3d transition metal molecules, while in our study here, B97-1 is demonstrated to be the second best method (on average) of all 42 tested functionals in predicting the ABE for 70 compounds chosen to have the most reliable data.

Some databases have been constructed to illustrate the performance of the DFT functionals in predicting some specific properties of molecules. We recently presented a comprehensive review on the accuracy of xc functionals across a broad spectrum databases in chemistry and physics,¹³ and 19 of the 24 highest ranked functionals in Table 4 were also included in the broad tests of ref 13. Here we list these 19 functionals in Table 9 where their performance on the 3dBE70 database is compared to their performance on three other databases:

- HTBH38: a database of 38 barrier heights of hydrogen atom transfer reactions,
- ABDE12: a database of 12 alkyl bond dissociation energies
- PPSS: a database of 5 π - π stacking energies

Table 9 also includes B3LYP because of its great historical popularity. The final column lists the sum of the four MUEs, and the 20 functionals are arranged in order of performance on this sum. Functionals near the top of this table have broad across-the-board performance. We find that the six functionals that perform worse than B3LYP all have 10% or less of Hartree–Fock exchange, but two functionals with zero Hartree–Fock exchange appear in the first five lines of the table, so Hartree–Fock exchange is but one part of the story. The performance of τ -HCTHhyb in Table 9 is particularly disappointing since it did so well for metal–ligand bond energies.

Of course the precise ranking of functionals depends on which databases one considers, but the main purpose of Table 9 is to show that the functionals that perform best in a broad assessment are not necessarily the ones that perform best on any one database. It is mildly discouraging that some of those that perform best on 3dBE70 alone do poorly in this broader

assessment. The quest for a universal functional continues, but data such as those presented here will allow us to assess progress as we move forward.

6. CONCLUSIONS

Due in part to the complication of near-degeneracy correlation and due also to the necessity to treat s and d electrons on an even footing, calculations of 3d transition-metal-containing compounds are still quite a challenge for theoretical chemistry. In the present investigation, 42 density functional approximations are tested against a database consisting of 70 molecules with experimental uncertainties of the enthalpy of formation equal to or less than 2.0 kcal/mol. The tested functionals include LSDA, GGAs, an NGA, global-hybrid GGAs, meta-GGAs, a meta-NGA, range-separated hybrid GGAs, global-hybrid meta-GGAs, a range-separated hybrid meta-GGA, a range-separated hybrid meta-NGA, and four examples of DFT-D. The Hartree–Fock method is included as well since it can be viewed as a special density functional with 100% HF exchange. The molecules in the database include all ten 3d transition metals and also involve diverse varieties of bond types ranging from the simple diatomic molecules to organometallics such as $\text{Sc}(\text{C}_5\text{H}_5)_3$.

We use the change of Born–Oppenheimer equilibrium atomization energy per bond as the reference quantity rather than the heat of formation because this removes dependence on elements in their solid-state standard states. The assessment of the accuracy of a functional is made by considering the mean unsigned error (MUE) in the atomization energy per bond, and the mean signed error is also calculated to show whether the average bond energy is overestimated or underestimated, which is very important for development of new approximations.

The following conclusions are worth repeating:

i) Averaged over the entire database, τ -HCTHhyb and B97-1 predict the most accurate bond energies among all the tested xc functionals. MPW1B95 gives the best result for SR molecules among all 42 functionals, and τ -HCTHhyb affords the best prediction for MR molecules.

ii) Local functionals, i.e., those with no Hartree–Fock exchange, are favored for computational work on very large systems because of their relatively low expense. The most accurate local functionals are the relatively recent OreLYP followed by OLYP, M06-L, and τ -HCTH plus two functionals (ω B97X-D and PW6B95-D3(BJ)) with molecular mechanics terms.

iii) Adding a dependence on kinetic energy densities can benefit both GGAs and the NGA xc functional.

iv) The M-H and M-O bond types are most the difficult to treat; this may result from significant MR characteristics.

v) Among the transition metals, the middle ones (V, Cr, and Mn) are harder to treat, on average, than either the early or late transition metals.

vi) The functionals that do best for metal–ligand bond energies do not necessarily do well for other quantities such as barrier heights, alkyl group bond energies, and π – π interactions.

AUTHOR INFORMATION

Corresponding Author

*E-mail: truhlar@umn.edu (D.G.T).

Notes

The authors declare no competing financial interest.

ACKNOWLEDGMENTS

The authors are grateful to Andy Luo for very helpful assistance. This work was supported in part by the Air Force Office of Scientific Research under grant number FA9550-11-1-0078, by the U.S. Department of Energy, Office of Basic Energy Sciences, Division of Chemical Sciences, Geosciences, and Biosciences under award DE-FG02-12ER16362, and by the Excellent Doctoral Dissertation Engagement Fund of Zhengzhou University in 2012.

REFERENCES

- (1) Kohn, W. *Rev. Mod. Phys.* **1999**, *71*, 1253–1266.
- (2) Kohn, W.; Sham, L. J. *Phys. Rev.* **1965**, *140*, A1133–A1138.
- (3) Raghavachari, K.; Anderson, J. B. *J. Phys. Chem.* **1996**, *100*, 12960–12973.
- (4) Barden, C. J.; Rienstra-Kiracofe, J. C.; Schaefer, H. F. *J. Chem. Phys.* **2000**, *113*, 690–700.
- (5) Yanagisawa, S.; Tsuneda, T.; Hirao, K. *J. Chem. Phys.* **2000**, *112*, 545–553.
- (6) Yanagisawa, S.; Tsuneda, T.; Hirao, K. *J. Comput. Chem.* **2001**, *22*, 1995–2009.
- (7) Baker, J.; Pulay, P. *J. Comput. Chem.* **2003**, *24*, 1184–1191.
- (8) Wu, Z. J. *Chem. Phys. Lett.* **2004**, *383*, 251–255.
- (9) Schultz, N. E.; Zhao, Y.; Truhlar, D. G. *J. Phys. Chem. A* **2005**, *109*, 4388–4403.
- (10) Schultz, N. E.; Zhao, Y.; Truhlar, D. G. *J. Phys. Chem. A* **2005**, *109*, 11127–11143.
- (11) Furche, F.; Perdew, J. P. *J. Chem. Phys.* **2006**, *124*, 044103.
- (12) Zhao, Y.; Truhlar, D. G. *J. Chem. Phys.* **2006**, *124*, 224105.
- (13) Peverati, R.; Truhlar, D. G. *Phil. Trans. Roy. Soc. A* **2013**, in press. Available at <http://arxiv.org/abs/1212.0944> (accessed July 19, 2013).
- (14) For a review of additional validation tests, see: Cramer, C. J.; Truhlar, D. G. *Phys. Chem. Chem. Phys.* **2009**, *11*, 10757–10816.
- (15) Jiang, W.; DeYonker, N. J.; Determan, J. J.; Wilson, A. K. *J. Phys. Chem. A* **2011**, *116*, 870–885.
- (16) Gáspár, R. *Acta Phys. Hung.* **1974**, *35*, 213.
- (17) Vosko, S. H.; Wilk, L.; Nusair, M. *Can. J. Phys.* **1980**, *58*, 1200–1211.
- (18) Becke, A. D. *Phys. Rev. A* **1988**, *38*, 3098–3100.
- (19) Lee, C.; Yang, W.; Parr, R. G. *Phys. Rev. B* **1988**, *37*, 785–789.
- (20) Handy, N. C.; Cohen, A. J. *Mol. Phys.* **2001**, *99*, 403–412.
- (21) Thakkar, A. J.; McCarthy, S. P. *J. Chem. Phys.* **2009**, *131*, 134109.
- (22) Perdew, J. P.; Burke, K.; Ernzerhof, M. *Phys. Rev. Lett.* **1996**, *77*, 3865–3868.
- (23) Zhao, Y.; Truhlar, D. G. *J. Chem. Phys.* **2008**, *128*, 184109.
- (24) Peverati, R.; Zhao, Y.; Truhlar, D. G. *J. Phys. Chem. Lett.* **2011**, *2*, 1991–1997.
- (25) Peverati, R.; Truhlar, D. G. *J. Chem. Theory Comput.* **2012**, *8*, 2310–2319.
- (26) Zhao, Y.; Truhlar, D. G. *J. Chem. Phys.* **2006**, *125*, 194101.
- (27) Peverati, R.; Truhlar, D. G. *J. Phys. Chem. Lett.* **2011**, *3*, 117–124.
- (28) Perdew, J. P.; Ruzsinszky, A.; Csonka, G. I.; Constantin, L. A.; Sun, J. *Phys. Rev. Lett.* **2009**, *103*, 026403.
- (29) Boese, A. D.; Handy, N. C. *J. Chem. Phys.* **2002**, *116*, 9559–9569.
- (30) Peverati, R.; Truhlar, D. G. *Phys. Chem. Chem. Phys.* **2012**, *14*, 13171–13174.
- (31) Adamo, C.; Barone, V. *Chem. Phys. Lett.* **1997**, *274*, 242–250.
- (32) Stephens, P. J.; Devlin, F. J.; Chabalowski, C. F.; Frisch, M. J. *J. Phys. Chem.* **1994**, *98*, 11623–11627.
- (33) Hamprecht, F. A.; Cohen, A. J.; Tozer, D. J.; Handy, N. C. *J. Chem. Phys.* **1998**, *109*, 6264–6271.
- (34) Keal, T. W.; Tozer, D. J. *J. Chem. Phys.* **2005**, *123*, 121103.
- (35) Hoe, W.-M.; Cohen, A. J.; Handy, N. C. *Chem. Phys. Lett.* **2001**, *341*, 319–328.
- (36) Adamo, C.; Barone, V. *J. Chem. Phys.* **1999**, *110*, 6158–6170.
- (37) Peverati, R.; Truhlar, D. G. *J. Chem. Phys.* **2011**, *135*, 191102.

- (38) Zhao, Y.; Schultz, N. E.; Truhlar, D. G. *J. Chem. Phys.* **2005**, *123*, 161103–161104.
- (39) Zhao, Y.; Schultz, N. E.; Truhlar, D. G. *J. Chem. Theory Comput.* **2006**, *2*, 364–382.
- (40) Zhao, Y.; Truhlar, D. *Theor. Chem. Acc.* **2008**, *120*, 215–241.
- (41) Zhao, Y.; Truhlar, D. G. *J. Chem. Theory Comput.* **2008**, *4*, 1849–1868.
- (42) Zhao, Y.; Truhlar, D. G. *J. Phys. Chem. A* **2004**, *108*, 6908–6918.
- (43) Zhao, Y.; Truhlar, D. G. *J. Phys. Chem. A* **2005**, *109*, 5656–5667.
- (44) Staroverov, V. N.; Scuseria, G. E.; Tao, J.; Perdew, J. P. *J. Chem. Phys.* **2003**, *119*, 12129–12137.
- (45) Heyd, J.; Scuseria, G. E.; Ernzerhof, M. *J. Chem. Phys.* **2003**, *118*, 8207–8215.
- (46) Henderson, T. M.; Izmaylov, A. F.; Scalmani, G.; Scuseria, G. E. *J. Chem. Phys.* **2009**, *131*, 044108.
- (47) Chai, J.-D.; Head-Gordon, M. *J. Chem. Phys.* **2008**, *128*, 084106.
- (48) Peverati, R.; Truhlar, D. G. *Phys. Chem. Chem. Phys.* **2012**, *14*, 16187–16191.
- (49) Peverati, R.; Truhlar, D. G. *J. Phys. Chem. Lett.* **2011**, *2*, 2810–2817.
- (50) (a) Grimme, S.; Antony, J.; Ehrlich, S.; Krieg, H. *J. Chem. Phys.* **2010**, *132*, 154104. (b) Grimme, S.; Ehrlich, S.; Goerigk, L. *J. Comput. Chem.* **2011**, *32*, 1456–1465.
- (51) Chai, J.-D.; Head-Gordon, M. *Phys. Chem. Chem. Phys.* **2008**, *10*, 6615–6620.
- (52) Yang, K.; Peverati, R.; Truhlar, D. G.; Valero, R. *J. Chem. Phys.* **2011**, *135*, 044118–044122.
- (53) Luo, S.; Truhlar, D. G. *J. Chem. Theory Comput.* **2012**, *8*, 4112–4126.
- (54) Mayhall, N. J.; Raghavachari, K.; Redfern, P. C.; Curtiss, L. A. *J. Phys. Chem. A* **2009**, *113*, 5170–5175.
- (55) DeYonker, N. J.; Peterson, K. A.; Steyl, G.; Wilson, A. K.; Cundari, T. R. *J. Phys. Chem. A* **2007**, *111*, 11269–11277.
- (56) DeYonker, N. J.; Williams, T. G.; Imel, A. E.; Cundari, T. R.; Wilson, A. K. *J. Chem. Phys.* **2009**, *131*, 024106.
- (57) Riley, K. E.; Merz, K. M. *J. Phys. Chem. A* **2007**, *111*, 6044–6053.
- (58) Li, S.; Dixon, D. A. *J. Phys. Chem. A* **2008**, *112*, 6646–6666.
- (59) Li, S.; Hennigan, J. M.; Dixon, D. A.; Peterson, K. A. *J. Phys. Chem. A* **2009**, *113*, 7861–7877.
- (60) Wang, T.-H.; Navarrete-López, A. M.; Li, S.; Dixon, D. A.; Gole, J. L. *J. Phys. Chem. A* **2010**, *114*, 7561–7570.
- (61) Li, S.; Dixon, D. A. *J. Phys. Chem. A* **2010**, *114*, 2665–2683.
- (62) Curtiss, L. A.; Raghavachari, K.; Redfern, P. C.; Pople, J. A. *J. Chem. Phys.* **1997**, *106*, 1063–1079.
- (63) Yungman, V. S. *Thermal Constants of Substances*; John Wiley & Sons, Inc.: New York, 1999; Vol. 5.
- (64) Mallard, W. G.; Linstrom, P. J. *NIST Chemistry WebBook*; NIST Standard Reference Database, Gaithersburg, MD, 2000. <http://webbook.nist.gov/chemistry/> (accessed November 1, 2011).
- (65) Chase, J. M. W.; Davies, C. A.; Downey, J. J. R.; Frurip, D. J.; McDonald, R. A.; Syverud, A. N. *NIST-JANAF Tables. J. Phys. Chem. Ref. Data, Monogr.*; 4th ed.; 1998; Vol. 9, pp 1–1952.
- (66) (a) Frisch, M. J.; Trucks, G. W.; Schlegel, H. B.; Scuseria, G. E.; Robb, M. A.; Cheeseman, J. R.; Scalmani, G.; Barone, V.; Mennucci, B.; Petersson, G. A.; Nakatsuji, H.; Caricato, M.; Li, X.; Hratchian, H. P.; Izmaylov, A. F.; Bloino, J.; Zheng, G.; Sonnenberg, J. L.; Hada, M.; Ehara, M.; Toyota, K.; Fukuda, R.; Hasegawa, J.; Ishida, M.; Nakajima, T.; Honda, Y.; Kitao, O.; Nakai, H.; Vreven, T.; Montgomery, J. A., Jr.; Peralta, J. E.; Ogliaro, F.; Bearpark, M.; Heyd, J. J.; Brothers, E.; Kudin, K. N.; Staroverov, V. N.; Kobayashi, R.; Normand, J.; Raghavachari, K.; Rendell, A.; Burant, J. C.; Iyengar, S. S.; Tomasi, J.; Cossi, M.; Rega, N.; Millam, J. M.; Klene, M.; Knox, J. E.; Cross, J. B.; Bakken, V.; Adamo, C.; Jaramillo, J.; Gomperts, R.; Stratmann, R. E.; Yazyev, O.; Austin, A. J.; Cammi, R.; Pomelli, C.; Ochterski, J. W.; Martin, R. L.; Morokuma, K.; Zakrzewski, V. G.; Voth, G. A.; Salvador, P.; Dannenberg, J. J.; Dapprich, S.; Daniels, A. D.; Farkas, Ö.; Foresman, J. B.; Ortiz, J. V.; Cioslowski, J.; Fox, D. J. *Gaussian 09*, Revision C.01; Gaussian, Inc.: Wallingford, CT, 2010. (b) Zhao, Y.; Peverati, R.; Yang, K.; Luo, S.; Truhlar, D. G. *MN-GFM*, version 6.5; University of Minnesota: Minneapolis, MN, 2013.
- (67) Alecu, I. M.; Zheng, J.; Zhao, Y.; Truhlar, D. G. *J. Chem. Theory Comput.* **2010**, *6*, 2872–2887.
- (68) Jiang, W.; Laury, M. L.; Powell, M.; Wilson, A. K. *J. Chem. Theory Comput.* **2012**, *8*, 4102–4111.
- (69) Zhao, Y.; Peverati, R.; Yang, K.; Truhlar, D. G. Minnesota Density Functionals Module 6.4, MN-GFM 6.4. See <http://comp.chem.umn.edu/mn-gfm/> for details (accessed July 19, 2013).
- (70) Weigend, F.; Ahlrichs, R. *Phys. Chem. Chem. Phys.* **2005**, *7*, 3297–3305.
- (71) Zheng, J.; Xu, X.; Truhlar, D. *Theor. Chem. Acc.* **2011**, *128*, 295–305.
- (72) Xu, X.; Truhlar, D. G. *J. Chem. Theory Comput.* **2011**, *7*, 2766–2779.
- (73) Ziegler, T.; Li, J. *Can. J. Chem.* **1994**, *72*, 783–789.